Geophysical Research Letters

RESEARCH LETTER
10.1029/2018GL079614

Seasonal Meandering of the Polar Front Upstream of the Kerguelen Plateau

E. Pauthenet[1], F. Roquet[1,2], G. Madec[3], C. Guinet[4], M. Hindell[5,6], C. R. McMahon[5,7,8], R. Harcourt[8], and D. Nerini[9]

[1]Department of Meteorology (MISU), Stockholm University, Stockholm, Sweden, [2]Department of Marine Sciences, University of Gothenburg, Gothenburg, Sweden, [3]LOCEAN Sorbonne Universitées (UPMC, University Paris 6)/CNRS/IRD/MNHN, Paris, France, [4]Centre d'Etudes Biologiques de Chizé, Centre National de la Recherche Scientifique, Villiers en Bois, Paris, France, [5]Institute for Marine and Antarctic Studies, University of Tasmania, Hobart, Tasmania, Australia, [6]Antarctic Climate and Ecosystem Cooperative Research Centre, University of Tasmania, Hobart, Tasmania, Australia, [7]Sydney Institute of Marine Science, Mosman, New South Wales, Australia, [8]Department of Biological Sciences, Macquarie University, Sydney, New South Wales, Australia, [9]Aix-Marseille Université, CNRS/INSU, Université de Toulon, IRD, Mediterranean Institute of Oceanography UM 110, Marseille, France

Key Points:
- A novel method classifying TS profiles reveals the spatiotemporal variability of the Polar Front (PF) in the Southern Indian Ocean
- West of the Kerguelen Plateau, the Polar Front follows the 49 degrees south latitude in the Austral spring, while in the autumn it is located at 53 degrees south
- This seasonal meandering covaries with the transport over the Plateau, suggesting important variations in circulation pathways

Supporting Information:
- Supporting Information S1

Correspondence to:
E. Pauthenet,
etienne.pauthenet@misu.su.se

Citation:
Pauthenet, E., Roquet, F., Madec, G., Guinet, C., Hindell, M., McMahon, C. R. et al. (2018). Seasonal meandering of the Polar Front upstream of the Kerguelen Plateau. *Geophysical Research Letters*, *45*, 9774–9781. https://doi.org/10.1029/2018GL079614

Received 13 JUL 2018
Accepted 19 AUG 2018
Accepted article online 27 AUG 2018
Published online 25 SEP 2018
Corrected 21 NOV 2018

This article was corrected on 21 NOV 2018. See the end of the full text for details.

Abstract The location of the Antarctic Polar Front (PF) is mapped in the Southern Indian Ocean by decomposing the shape of temperature and salinity profiles into vertical modes using a functional Principal Component Analysis. We define the PF as the northernmost minimum of temperature at the subsurface and represent it as a linear combination of the first three modes. This method is applied on an ocean reanalysis data set and on in situ observations, revealing a seasonal variability of the PF latitudinal position that is most pronounced between the Conrad Rise and the Kerguelen Plateau. This shift coincides with variations in the transport across the Northern Kerguelen Plateau. We suggest that seasonal changes of the upper stratification may drive the observed variability of the PF, with potentially large implications for the pathways and residence time of water masses over the plateau and the phytoplankton bloom extending southeast of the Kerguelen Islands.

Plain Language Summary The Antarctic Polar Front (PF) is a water mass boundary that flows around Antarctica between approximately 48°S and 56°S in the Southern Indian Ocean. The position of the PF in space and time is important to understand the oceanic circulation, the heat and salt exchanges, and also marine ecosystems. In the Indian sector the PF has to cross the Kerguelen Plateau, a major bottom topography feature. The present study develops and then applies a novel method for mapping the PF taking into account the whole hydrographic structure in the upper 300 m of the ocean. We are able to map the PF position and find that it presents large seasonal variations that are more intense just west of the Kerguelen Plateau. Between the Conrad Rise and the Kerguelen Plateau, the PF is essentially zonally orientated in September and found farther south by up to 4° latitude in March. Shifts in the PF position are shown to correlate with a seasonal variation in volume transport between Kerguelen and Heard Islands. We discuss how these seasonal variations in circulation pathways could have an impact on the local marine ecosystems.

1. Introduction

The Southern Ocean circulation is dominated by the wind-driven Antarctic Circumpolar Current (ACC) flowing eastward and organized in three major fronts that influence the general water mass distribution. Most of the flow is carried by the well-defined Subantarctic Front (SAF), while the Southern ACC Front (SACCF) stands as the southernmost dynamic ACC front. In between lies the Antarctic Polar Front (PF) from 48 to 56°S in the Southern Indian Ocean (0–130°E; Orsi et al., 1995). The PF is typically defined as the northernmost extent of the Winter Water and denotes the northern limit of salinity control on the stratification, allowing a temperature minimum (T-min) at the subsurface to develop south of the PF (Pollard et al., 2002). The location of the PF around Kerguelen has been studied previously (e.g., Park et al., 2014), yet there remains much uncertainty especially in the region to the west of Kerguelen Islands (30 to 75°E; Figure 6b in ; Kim & Orsi, 2014). We recapitulate the main previous mapping of the PF together with a companion table containing the methodologies and limitations of these studies (Figure and Table S1 in the supporting information).

In the present study we propose a new way to identify the PF using a powerful dimension reduction method. Previously, Pauthenet et al. (2017) analyzed the thermohaline structure of the Southern Ocean and they showed that variations in the vertical shape of the Southern Ocean temperature (T) and salinity (S) profiles down to 2,000 m could be reduced to two vertical modes that account for more than 90% of the observed variability. The distribution of these low vertical modes can be linked to the spatiotemporal variations of the major Southern Ocean frontal positions. Using this method, we objectively analyze the shape of T and S profiles from 5 to 300 m from a reanalysis and in situ observations and propose a robust definition of the PF. The position of the inferred PF is then discussed in relation with the transport across the plateau. It is shown that this new method efficiently maps the PF and gives new insights on the seasonal and interannual variability of its position in the vicinity of Kerguelen.

2. Data and Methods

We apply a transformation technique on T and S profiles coined functional principal component analysis (fPCA) in the multivariate case (Berrendero et al., 2011; Ramsay & Silverman, 2005). The source code used for the analysis is available as an R package via Github (https://github.com/EPauthenet/fda.oce). In this section we briefly describe the data sets and methods used and we refer the reader to Pauthenet et al. (2017) for further details on applying fPCA to a collection of T and S profiles.

2.1. Reanalysis Data

The profiles used to compute the vertical modes are T and S profiles from the Global Ocean Reanalysis (GLORYS, GLOBAL_REANALYSIS_PHY_001_025; Ferry et al., 2016). This product is a reanalysis of the ocean state obtained by constraining the Nucleus for European Modelling of the Ocean ocean model at 1/4° resolution with in situ T and S profiles including Array for Real-Time Geostrophic Oceanography (ARGO) and Marine Mammals Exploring the Oceans Pole to Pole (MEOP) profiles, satellite sea surface temperature, and along-track sea level anomalies. We found that the subsurface temperature in the GLORYS field is misrepresented in the PF region before 2007, probably due to the lack of in situ observations to constrain the model (Figure S2). Thus, we analyze the ~10 million monthly mean T and S profiles, in the Southern Indian Ocean (0 to 130°E and 40 to 70°S) for the period 2007–2014 only. We also compute time series of the transport over the plateau by integrating the GLORYS zonal velocity field from the Antarctic coast toward the north. This gives stream function fields, and the difference of these values between Heard (53.1°S, 73.3°E) and Kerguelen (49.7°S, 70.1°E) islands is taken as the bulk transport over the northern plateau.

2.2. Decomposition of the Thermohaline Structure

The goal is to analyze the shape of T and S profiles and their joint variations. The method requires profiles of fixed depth. Here we are constrained by the shallow bathymetry over the plateau, so we apply the method to profiles of depth 5 to 300 m which corresponds to the first 35 vertical levels of the GLORYS grid. The T and S profiles are first expressed as a linear superposition of B-splines functions. This step normalizes the profiles from any observational platform or models. We choose a number of $K = 20$ B-splines per profiles corresponding to an effective resolution of 15 m by spline. B-spline coefficients are stored in a table $N \times (2K)$ with each observation being the K coefficients for T and S profiles joined end to end. The fPCA then decomposes this table into principal components (PCs), that is, uncorrelated linear combinations of the original variables, that maximize the variance. The vertical modes of the Southern Indian Ocean are computed on the T and S profiles from GLORYS (2007–2014). These modes define a basis on which any T and S profile can be projected. It is thereafter possible to reconstruct the truncated $T^{(q)}$ and $S^{(q)}$ profiles by summing the q first eigen functions ($\{\xi_k^T(z), \xi_k^S(z)\}$) weighted by their respective PC values (y_n^k) as follows:

$$\begin{cases} T_n^{(q)}(z) = \overline{T}(z) + \sum_{k=1}^{q} y_{n,k}\xi_k^T(z) \\ S_n^{(q)}(z) = \overline{S}(z) + \sum_{k=1}^{q} y_{n,k}\xi_k^S(z) \end{cases} \quad (1)$$

with the $n = 1, \ldots, N$ profile index, $k = 1, \ldots, K$ the mode numbers, $z \in \{5, 300\}$ m the depth, and $\{\overline{T}, \overline{S}\}$ the mean reference T and S profiles. For readability, the PC values are noted PC1, PC2, etc … in the text and figures, and y_1, y_2, etc … in the equations.

2.3. Polar Front Detection

We rely on the phenomenological indicator of the PF that is the northernmost position of a subsurface T-min (Botnikov, 1963) and define the separation in the PC space that corresponds to it. The existence of a subsurface T-min implies the presence of a gradient inversion in T between the subsurface and deeper waters. When this gradient is positive (negative) downward, the subsurface T-min (does not) exists and the profile is located south (north) of the PF. The criterion is thus recasted into a condition on the T gradient.

Different values for the subsurface depth have been tested on several in situ sections, and it was found that values between 150 and 170 m gives similar results, so we use 160 m as the subsurface depth. To identify the limit of the PF in the PC space, we use the truncated T profiles of order $q = 3$ (equation (1), for ranges of PC values spanning the Polar Front Zone (between the SAF and the PF) and Antarctic Zone (between the PF and the Southern Boundary). Thus, the sign of the vertical T gradient between 160 and 300 m is then associated to PC values. The boundary between the two zones corresponds to a plane in the PC1/PC2/PC3 space of equation $C_{PF} = ay_1 + by_2 + cy_3 + d$ such that the norm of the T vertical gradient between 160 and 300 m is minimized. The criterion is then simply $C_{PF} = 0$ at the PF, $C_{PF} < 0$ for profiles showing a T-min at the subsurface (i.e., south of the PF) and $C_{PF} > 0$ for the homogeneous profiles of the Polar Front Zone (i.e., north of the PF). Note that coefficients of the polynomial C_{PF} depend on the actual fPCA eigen modes; however, they rely on an underlying assumption independent of the method of decomposition.

2.4. In Situ Data

The PF detection is validated by projecting in-situ MEOP (Roquet et al., 2018) and ARGO (Argo, 2000) profiles on the fPCA basis. Since 2004, elephant seals have been equipped with high-accuracy conductivity-temperature-depth satellite-relayed data loggers providing T and S profiles along their tracks (Treasure et al., 2017). Here we use the profiles that have been interpolated on a regular vertical grid (1-dbar spacing) from the MEOP-conductivity-temperature-depth database (version 2017-11-11). We found 54,667 MEOP profiles extending from 5 to at least 300 m deep in our study area over the 2007–2017 period. One key advantage of this data set is the availability of finely resolved sections across the PF at different times of the year (Roquet et al., 2009) that will be used to assess the robustness of our criterion.

ARGO profiling floats measure the temperature and salinity of the upper 2,000 m of the World Ocean (Riser et al., 2016). They constitute the main source of hydrographic profiles nowadays, including in the Southern Ocean north of 60°S. We use the 77,934 ARGO profiles sampled over the 2007–2017 period in the study area.

3. Results

3.1. Vertical Modes

The first three vertical modes are sufficient to describe 97% of the variance, a value similar to the one found for the whole Southern Ocean (96%; Pauthenet et al., 2017). The average spatial distributions of the two main PCs are presented in Figures 1a and 1b, and the vertical shape of the modes is shown in Figure 1c.

The first vertical mode accounts for 73% of the variance and captures the general gradient of warming and saltening of the water column with increasing latitude, marking the SAF sharply (Figure 1a). The variations of T and S explained by the first mode are homogenous down to 300 m (Figure 1c). A positive (negative) PC1 corresponds to warmer (colder) and saltier (fresher) waters, with slightly less salinity stratified waters for a positive PC1 (Figure 1c). T and S contribute almost equally to this PC (57% and 43%, respectively). The second mode (21%, Figure 1b) is driven primarily by salinity (65%). High positive PC2 values correspond to colder waters at all depths (Figure 1c). The effect of PC2 on salinity is larger at 300 m than at the surface and is opposite in shape to that of the effect of PC1 on salinity (Figure 1c). It means that positive PC2 values correspond to more salinity stratified waters. The spatial distribution of PC3 (Figure S3c) presents a positive blob over the Northern Kerguelen Plateau (PC3 > 0.2). PC3 accounts for a smaller variance (3%) and is mainly driven by salinity (90%) in the upper 100 m (Figures S3a and S3b).

The distribution of T and S profiles in PC1/PC2 space is shown in Figure 1d, featuring a Z-shape typical of the Southern Ocean corresponding to (from left to right) the Antarctic continental margin, the Antarctic Zone, and the convergence zone north of the PF. The first two PCs covary north of the PF and in the Antarctic continental margin (Figure 1d). However, in the Antarctic Zone, PC1 is almost constant and PC2 reveals additional structures such as the intense Fawn Trough current (Roquet et al., 2009) across the Kerguelen Plateau and contours following the SACCF.

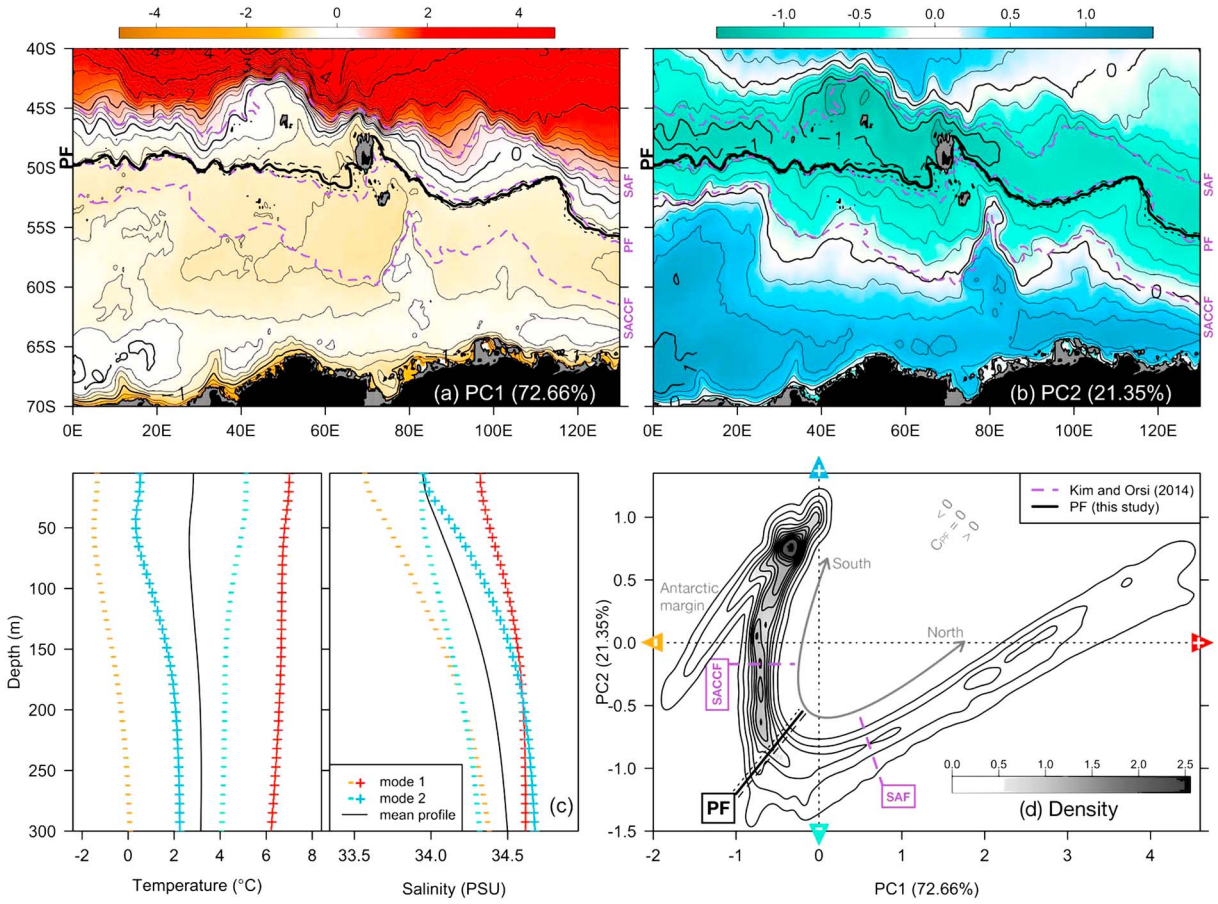

Figure 1. The PF is a transition between PC1 and PC2 as illustrated by their mean spatial distribution (a) and (b) based on GLORYS (2007–2014), with a 0.25 contour interval. The PF is represented by the contour of $C_{PF} = 0$ (black bold) and $C_{PF} = \pm 0.05$ (black dashed, +0.05, and dotted, −0.05). Climatological SAF, PF, and SACCF from Kim and Orsi (2014) are added in purple dashed contours. (c) Representation of the effects of adding (+) and subtracting (-) the first two vertical modes ($\sqrt{\lambda_k}\xi_k$) on T and S mean profiles (black lines) (with λ^k the eigen values; see Pauthenet et al., 2017). (d) Two-dimensional kernel density estimate of the mean PC1 and PC2 values, with a 0.2 contour interval. The PF criterion is represented as a black segment with the range ± 0.05 in dashed and dotted lines. The SAF and SACCF are represented as segments of $y_2 = -0.17$ and $y_2 = -2y_1 + 0.04$, respectively, visually corresponding to the fronts of Kim and Orsi (2014) in the maps (a) and (b). PC3 map and vertical modes are shown in Figure S3. PF = Polar Front; SAF = Subantarctic Front; SACCF = Southern ACC Front; PSU = practical salinity unit.

3.2. Polar Front Position and Variability

The coefficients of the plane (see section 2.4) defining the PF criterion are $C_{PF} = 0.82y_1 - y_2 + 0.16y_3 - 0.38$ (Figures 1a, 1b, and 2). It can be visualized as a segment ($y_2 = 0.82y_1 - 0.38$) on the space PC1/PC2 (Figure 1d). PC3 has been kept in the analysis because it provides a minor contribution in the vicinity of Kerguelen (Figure S3). The average subsurface (200 m) T and S values at the PF ($C_{PF} = 0$) are 2.61°C (±0.45 std) and 34.04 PSU (±0.06 std) over the 0 to 130°E longitude domain and the 2007–2014 period (Figure S4).

The PF presents a clear seasonal cycle that is amplified between the Conrad Rise and the Kerguelen Plateau before being constrained along the southeastern edge of the Kerguelen Islands (Figure 2a). During Austral autumn (March-April-May) the front is found farther south over the plateau (52 versus 47°S in September), advecting water northward from Heard Island to Kerguelen Island (Figure 2a). The seasonal magnitude of the PF latitude position (1.77 ± 1.21 std degree latitude) is larger than the interannual magnitude (1.05 ± 0.63 std degree latitude). The PF presents a nonsignificant interannual southward trend over the 2007–2014 period (3×10^{-3} latitude degree/year, p value= 0.317, Figure 2b).

We present the distribution of MEOP and ARGO in situ observations with the locations color coded according to their C_{PF} zs (Figure 2c). Note that the different products are not independent as the GLORYS reanalysis has been constrained by both ARGO and MEOP data. The PF is identified in yellow by $|C_{PF}| < 0.05$ to visualize the range of the spatial variations (Figure 2c). This range corresponds to an average temperature variation at

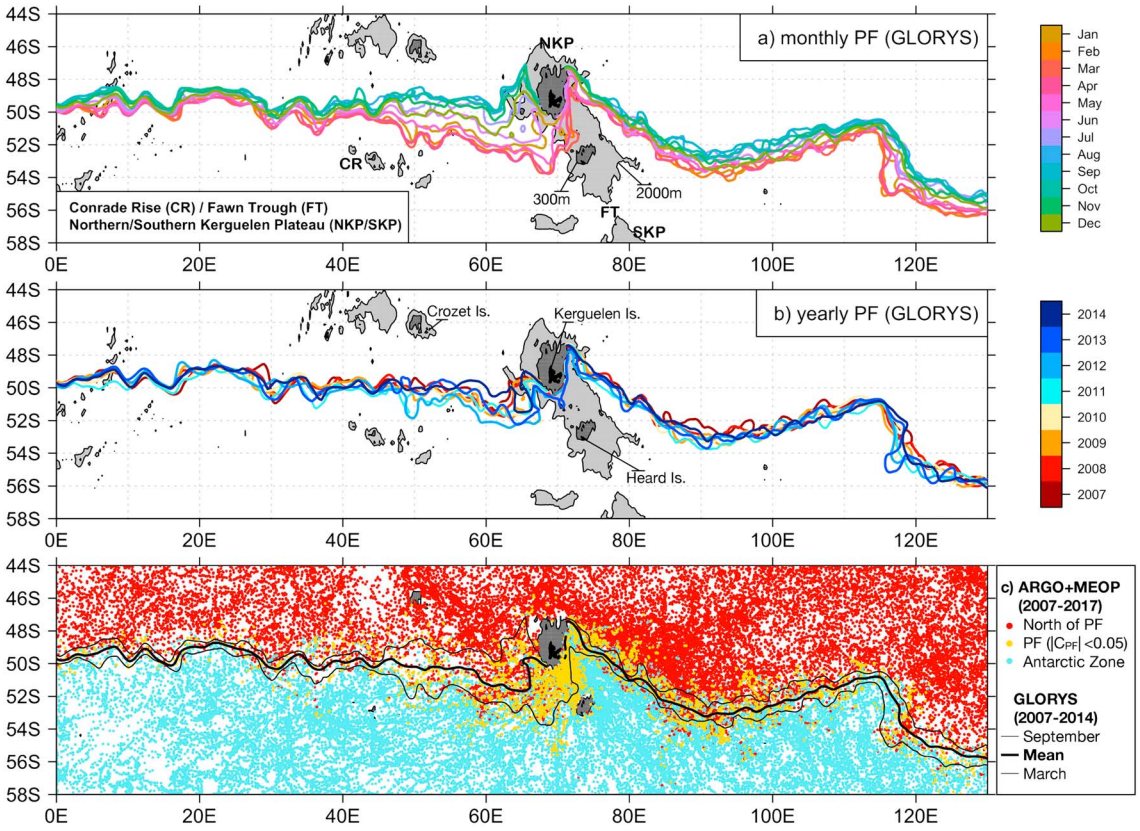

Figure 2. Maps of the PF latitudinal band in the Indian sector displaying (a) the monthly mean and (b) the annual mean PF position from GLORYS (2007–2014). The in situ profiles from ARGO and MEOP (c) for the period 2007–2017 are successfully classified with the same criterion. Note in (a) and (c) the large seasonal variation west of the Kerguelen Plateau and in (b) no significant shift of the PF over the period 2007–2014. PF = Polar Front; MEOP = Mammals Exploring the Oceans Pole to Pole; ARGO = Array for Real-Time Geostrophic Oceanography.

the surface of 0.37°C (±0.52 std) and an average latitude range of 0.31° ± (0.30 std). The largest spread of the ±0.05 limit is located west of Kerguelen, characteristic of a weaker water mass boundary (Figures 1a and 1b). The northernmost (September) and southernmost (March) extents of the GLORYS-based fronts are consistent with the in situ profiles classification (Figure 2c).

To investigate on the seasonal variations in PF position, we present two T and S sections from MEOP that extend south of Kerguelen in two different seasons (Figure 3). The sections are located along the 70°E meridian in April (returning to Kerguelen) and October (leaving Kerguelen) 2014. In April 2014, the GLORYS PF contour is located south of 52°S and is deflected north approaching the Kerguelen Plateau, which is visible in the northern part of section 1. The T-min at the subsurface is marked, and its northernmost limit ends around 52°S where the criterion C_{PF} changes sign (Figure 3a). In October 2014, the PF is not found south of Kerguelen as revealed in section 2 where C_{PF} values are negative for all profiles (Figure 3b). So in October 2014, the PF is either disrupted or located north of the Kerguelen Islands as the blue contour indicates in Figure 3g. Visual inspection of a large number of seal sections crossing the PF confirms the robustness of our method to detect the place where the T-min vanishes marking the position of the PF. Two further examples of sections confirm a northernmost position of the PF west of Kerguelen during the Austral summer (November 2011 and December 2009, Figure S5).

Associated with the seasonal shift in the location of the PF, we find a seasonal cycle in the transport between Heard and Kerguelen Islands, computed from the GLORYS velocity fields (Figure 4). This seasonal cycle is anti-correlated (−0.34) with the average latitude position of the PF between 60 and 70°E. The maximum mean transport (2.34 Sv) is in March, when the PF is southernmost (~52°S over the plateau, Figures 2 and 4). This transport has a median seasonal signature of 26% of its maximum amplitude (3.34 Sv on July 2012): in August the median transport is of 1.48 Sv (±0.83 std) compared to 2.34 Sv (±0.61 std) in March. The average transport

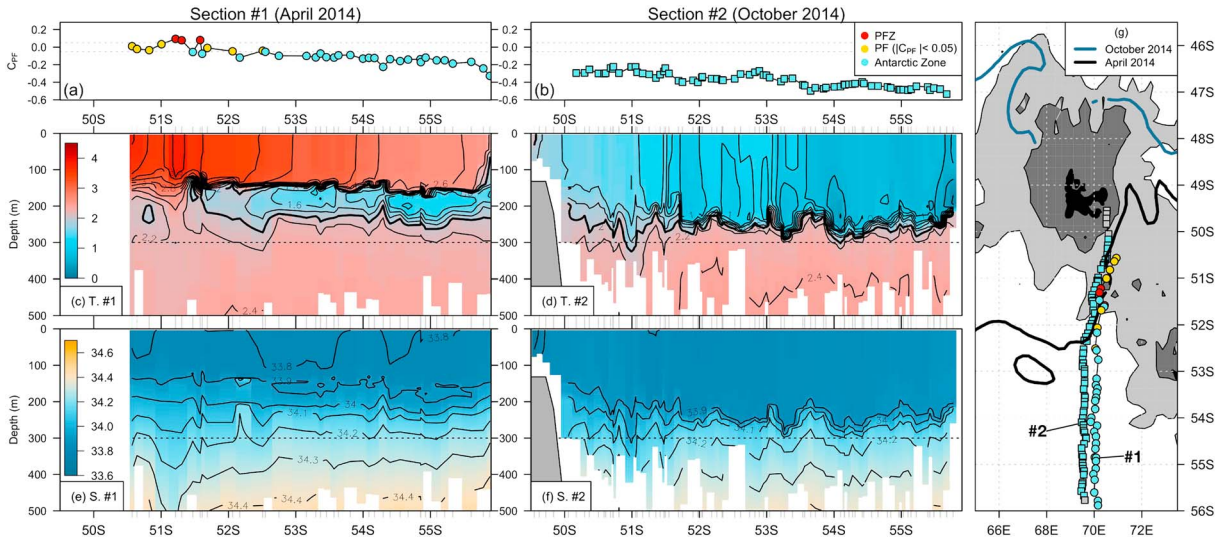

Figure 3. Example of two in situ MEOP sections that illustrate the spatial variability of the PF over the plateau. Section 1 (ct98-42-13) is sampled from 23 April 2014 to 5 May 2014 (April) and section 2 (ct112-047-14) from 20 October 2014 to 23 October 2014 (October). The panels (a) and (b) represent the criterion C_{PF} computed for each profile. The profiles are on the PF ($|C_{PF}|<0.05$, yellow dot), in the PFZ ($C_{PF}>0$, red dot), or in the Antarctic Zone ($C_{PF}<0$, blue dot). (c, d, e, and f) The T and S sampled along the tracks. Panel (g) is the map of the trajectories leaving (#2) Kerguelen and returning (#1) to Kerguelen. The contours are the PFs ($C_{PF}=0$) derived from GLORYS in October 2014 (blue) and April 2014 (black). MEOP = Mammals Exploring the Oceans Pole to Pole; PF = Polar Front; PFZ = Polar Front Zone.

estimated across the plateau over the period 2007–2014 (2.02 Sv ±0.57 std) is consistent with previous estimates (~2 Sv, Park et al., 2009).

4. Discussion and Conclusions

We used an objective method developed in Pauthenet et al. (2017) to decompose in modes the vertical structure of T and S profiles and locate the PF in the upper 300 m of the Southern Indian Ocean, between 2007 and 2014. The decomposition method we used is robust as it maximizes the use of available information from both T and S profiles instead of relying on a single depth criterion in standard hydrographic methods. A future goal would be to describe the circumpolar fronts of the Southern Ocean, either by looking for gradients in the PC maps or by defining criteria on T or S such as the one we developed here for the PF. The method is here applied to T and S profiles; however, it would be straightforward to include other properties in the decomposition (e.g., nutrients, chlorophyll, and oxygen) for biogeochemical applications.

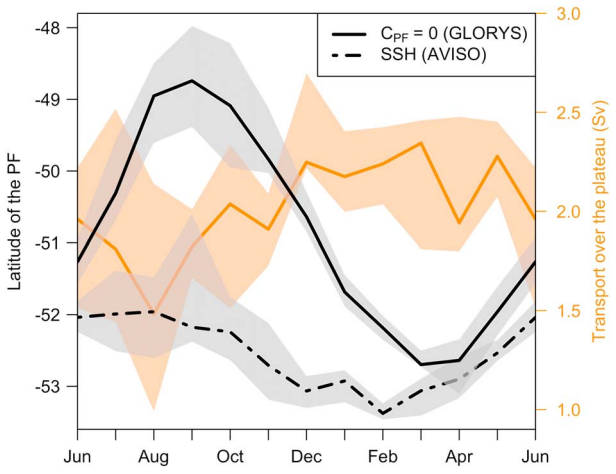

Figure 4. The transport between Heard and Kerguelen Islands (orange) computed from GLORYS is anticorrelated with the average PF latitude between 60 and 70°E (black). The PF latitudes from GLORYS (black full line) are estimated with our criterion $C_{PF}=0$, like plotted in Figure 2. The PF from the SSH field is estimated by selecting a contour of the AVISO field (AVISO, 2009), following Kim and Orsi (2014; black dashed lines). The lines are the medians, and the shadings are the 25% and 75% quartiles of the distributions of latitude and transport, for the period 2007–2014. PF = Polar Front; SSH = Sea Surface Height.

The PF is best seen as a bend in the T and S profiles distribution in the PC1/PC2 space (Figure 1d) supporting the idea that the PF marks a fundamental change of stratification within the Southern Ocean (Pollard et al., 2002). Our climatological PF is in best agreement with the studies of Kim and Orsi (2014) and Park et al., (2009, 2014; see Figure S1). The period 2007–2014 is too short to assess interannual variability, yet the PF presents no significant meridional shift in GLORYS which is consistent with several studies using surface gradients of sea surface height (SSH) (e.g., Chapman, 2017; Graham et al., 2012) but goes against the single SSH value criteria that identify a southward shift of the fronts (e.g., Kim & Orsi, 2014; Sokolov & Rintoul, 2009). A clear seasonal shift that is amplified between the Conrad Rise and the Kerguelen Plateau is documented. It was also described in Kim and Orsi (2014) as it is also captured by a SSH value criterion yet with a much weaker magnitude than in our analysis (Figure 4) suggesting once more that tracking the frontal positions with a unique SSH value works only approximately.

The correlation between the frontal position and the transport across the Kerguelen Plateau (Figure 4) suggests a role of the bottom topography in steering the PF. The region to the west of Kerguelen is prone to having large variations of velocity and direction between the surface and deep currents, which can be explained by considering Stommel's beta spiral (Hughes & Killworth, 1995) :

$$\partial_z \theta = -\frac{N^2 w}{f|\mathbf{u}|^2}, \tag{2}$$

with θ the angle of the geostrophic velocity vector $\mathbf{u}$, $N^2 = -(g/\rho_0)\partial_z \rho$ the Brunt-Väisälä frequency, f the Coriolis parameter, and w the vertical velocity. West of Kerguelen, the water masses are ascending the Kerguelen Plateau to bypass it, so $w > 0$, inducing a cyclonic (clockwise) spiral downward. As the current $\mathbf{u}$ is weak and the stratification is more intense in summer (i.e., higher N^2), the angle of the currents west of Kerguelen should vary more with depth, allowing surface currents to pass across or north of the plateau, while the deep currents skirt the plateau to the south. It is therefore expected that the summer stratification facilitates the seasonal shift of the PF in the first 300 m, being pushed south by warmer and fresher waters brought from the northwest by the ACC (Figures 3c and 3e). This regime of fresher and warmer water is well captured by PC2 and is visible as a patch of PC2< -1 values around Crozet and Kerguelen Islands (Figure 1b).

The large seasonality of the PF has various implications for the circulation, biogeochemistry, and ecology in the region that requires further investigation. Marine apex predators (penguins, albatrosses, and seals) are known to rely on the frontal zones for foraging (Bost et al., 2009). For example, the latitudinal position of the PF between 47 and 60°E is directly linked with the survival rate of the king penguin population from the Crozet Islands (Bost et al., 2015; Péron et al., 2012). Seasonal meandering of the PF may have significant implications on the foraging strategies of marine predators.The seasonal change in water mass pathways over the Kerguelen Plateau could be important for the transport of chemical elements on the plateau. Sanial et al. (2015) specifically found that chemical elements to the east of Kerguelen originated from the shelves of the Kerguelen Islands implying a transport of chemical elements across the PF. But in the Austral autumn our PF is advecting water northeastward between Heard and Kerguelen Islands, so these chemical elements may also be advected in part from the shelf of Heard Island.The seasonal meandering of the PF over the plateau can influence the large annual phytoplankton blooms (~45,000 km^2) southeast of the Kerguelen Islands, starting around November and then collapsing around February (Blain et al., 2007). This bloom is an important sink of CO_2, controlled by the natural iron fertilization of surface waters. The iron is essentially transferred from the bottom sediment of the plateau to the mixed layer by internal tides (Park et al., 2008) and a deep mixed layer which further favors the transfer. The observed seasonal shift of the PF is connected to local changes in stratification that may influence the mixed layer depth variations and the residence time over the plateau, thus shaping the distribution and timing of the bloom. Further investigation of the dynamics of the observed meandering of the PF is needed to fully comprehend the marine ecosystem over and east of the Kerguelen Plateau and assess how they might respond to ongoing climate changes.

Acknowledgments
This work was supported by the Bolin Center for Climate Research. Copernicus Marine Environment Monitoring Service (CMEMS) provided freely the GLORYS reanalysis (http://marine.copernicus.eu/services-portfolio/access-to-products/). The International ARGO Program provided freely the ARGO floats hydrographic data (accessible from the ifremer portal : ftp://ftp.ifremer.fr/ifremer/argo/). The marine mammal data were collected and made freely available (http://meop.net) by the International MEOP Consortium and the national programs that contribute to it, including the Integrated Marine Observing System (IMOS) for Australian data and Mammals as samplers of the Ocean Environment (MEMO) for French data. We thank Isabelle Durand and Yong Sun Kim for providing mean PF paths. Finally, we are grateful to two reviewers for their constructive criticisms and helpful suggestions on the manuscript.

References

Argo (2000). Argo float data and metadata from Global Data Assembly Centre (Argo GDAC). SEANOE. http://doi.org/10.17882/42182

AVISO (2009). Ssalto/duacs user handbook:(m) SLA and (m) ADT near-real time and delayed time products, Rep,CLS-DOS-NT, 6, 51.

Berrendero, J. R., Justel, A., & Svarc, M. (2011). Principal components for multivariate functional data. *Computational Statistics & Data Analysis*, *55*(9), 2619–2634. https://doi.org/10.1016/j.csda.2011.03.011

Blain, S., Quéguiner, B., Armand, L., Belviso, S., Bombled, B., Bopp, L., et al. (2007). Effect of natural iron fertilization on carbon sequestration in the Southern Ocean. *Nature*, *446*(7139), 1070.

Bost, C. A., Cotté, C., Bailleul, F., Cherel, Y., Charrassin, J. B., Guinet, C., et al. (2009). The importance of oceanographic fronts to marine birds and mammals of the Southern Oceans. *Journal of Marine Systems*, *78*(3), 363–376. https://doi.org/10.1016/j.jmarsys.2008.11.022

Bost, C. A., Cotte, C., Terray, P., Barbraud, C., Bon, C., Delord, K., et al. (2015). Large-scale climatic anomalies affect marine predator foraging behaviour and demography. *Nature Communications*, *6*, 8220.

Botnikov, V. (1963). Geographical position of the Antarctic convergence zone in the Antarctic Ocean. *Soviet Antarctic Expedition Information Bulletin*, *41*, 324–327.

Chapman, C. C. (2017). New perspectives on frontal variability in the Southern Ocean. *Journal of Physical Oceanography*, *47*(5), 1151–1168.

Ferry, N., Garric, G., Parent, L., Masina, L., Storto, S., Zuo, A. H., et al. (2016). CMEMS product user manual for global ocean reanalysis products, CMEMS-GLO-QUID-001-025, 3.5 ed.

Graham, R. M., Boer, A. M., Heywood, K. J., Chapman, M. R., & Stevens, D. P. (2012). Southern Ocean fronts: Controlled by wind or topography? *Journal of Geophysical Research*, *117*, C08018. https://doi.org/10.1029/2012JC007887

Hughes, C. W., & Killworth, P. D. (1995). Effects of bottom topography in the large-scale circulation of the Southern Ocean. *Journal of Physical Oceanography*, *25*(11), 2485–2497.

Kim, Y. S., & Orsi, A. H. (2014). On the variability of Antarctic Circumpolar Current fronts inferred from 1992–2011 altimetry. *Journal of Physical Oceanography*, *44*, 3054–3071.

Orsi, A. H., Whitworth III, T., & Nowlin Jr, W. D. (1995). On the meridional extent and fronts of the antarctic circumpolar current. *Deep-Sea Research Part I: Oceanographic Research Papers*, *42*(5), 641–673.
Park, Y., Durand, I., Kestenare, E., Rougier, G., Zhou, M., d'Ovidio, F., et al. (2014). Polar front around the Kerguelen Islands: An up-to-date determination and associated circulation of surface/subsurface waters. *Journal of Geophysical Research: Oceans*, *119*, 6575–6592. https://doi.org/10.1002/2014JC010061
Park, Y.-H., Fuda, J.-L., Durand, I., & Naveira Garabato, A. C. (2008). Internal tides and vertical mixing over the Kerguelen Plateau. *Deep-Sea Research Part II: Topical Studies in Oceanography*, *55*(5), 582–593.
Park, Y. H., Vivier, F., Roquet, F., & Kestenare, E. (2009). Direct observations of the ACC transport across the Kerguelen Plateau. *Geophysical Research Letters*, *36*, L18603. https://doi.org/10.1029/2009GL039617
Pauthenet, E., Roquet, F., Madec, G., & Nerini, D. (2017). A linear decomposition of the Southern Ocean thermohaline structure. *Journal of Physical Oceanography*, *47*(1), 29–47.
Péron, C., Weimerskirch, H., & Bost, C.-A. (2012). Projected poleward shift of king penguins'(Aptenodytes patagonicus) foraging range at the Crozet Islands, southern Indian Ocean. *Proceedings of the Royal Society of London B: Biological Sciences*, *279*, 2515–2523.
Pollard, R. T., Lucas, M. I., & Read, J. F. (2002). Physical controls on biogeochemical zonation in the Southern Ocean. *Deep-Sea Research Part II: Topical Studies in Oceanography*, *49*(16), 3289–3305.
Ramsay, J., & Silverman, B. (2005). *Functional data analysis*. New York: Springer.
Riser, S. C., Freeland, H. J., Roemmich, D., Wijffels, S., Troisi, A., Belbéoch, M., et al. (2016). Fifteen years of ocean observations with the global Argo array. *Nature Climate Change*, *6*(2), 145.
Roquet, F., Guinet, C., Charrassin, J.-B., Costa, D. P., Kovacs, K. M., Lydersen, C., et al. (2018). MEOP-CTD in-situ data collection: a Southern ocean Marine-mammals calibrated sea water temperatures and salinities observations. SEANOE. http://doi.org/10.17882/45461
Roquet, F., Park, Y. H., Guinet, C., Bailleul, F., & Charrassin, J. B. (2009). Observations of the fawn trough current over the Kerguelen Plateau from instrumented elephant seals. *Journal of Marine Systems*, *78*, 377–393.
Sanial, V., Van Beek, P., Lansard, B., Souhaut, M., Kestenare, É., d'Ovidio, F., et al. (2015). Use of Ra isotopes to deduce rapid transfer of sediment-derived inputs off Kerguelen. *Biogeosciences*, *12*(5), 1415–1430.
Sokolov, S., & Rintoul, S. R. (2009). Circumpolar structure and distribution of the Antarctic Circumpolar Current fronts: 1. Mean circumpolar paths. *Journal of Geophysical Research*, *114*, C11018. https://doi.org/10.1029/2008JC005108
Treasure, A. M., Roquet, F., Ansorge, I. J., Bester, M. N., Boehme, L., Bornemann, H., et al. (2017). Marine mammals exploring the oceans pole to pole. *Oceanography*, *30*(2), 62–68.

Erratum

In the originally published version of this article, an error was identified in section 4, the third paragraph. The sentence "West of Kerguelen, the water masses are ascending the to bypass it, so $w > 0$, inducing a cyclonic (clockwise) spiral downward." should have read "West of Kerguelen, the water masses are ascending the Kerguelen Plateau to bypass it, so $w > 0$, inducing a cyclonic (clockwise) spiral downward." This error has since been corrected, and this version may be considered the authoritative version of record.